Ultrasound in Med. & Biol. Vol. 16, No. 3, pp. 241–246, 1990
Printed in the U.S.A.

0301–5629/90 $3.00 + .00

Original Contribution

TISSUE RESPONSE TO MECHANICAL VIBRATIONS FOR "SONOELASTICITY IMAGING"

K. J. PARKER, S. R. HUANG, R. A. MUSULIN and R. M. LERNER
Rochester Center for Biomedical Ultrasound, University of Rochester, Rochester, New York 14627

(*Received* 3 *March* 1989; *in final form* 10 *August* 1989)

Abstract—The goal of "sonoelasticity imaging" is to differentiate between normal soft tissues and hard lesions. This is done by measuring and then displaying the ultrasound Doppler spectrum of regions within tissues which are mechanically forced with low frequency (20–1000 Hz) vibrations. The resolution and sensitivity of the technique ultimately rest on the spatial resolution of ultrasound Doppler detection, the low frequency mechanical properties of tissues, and the vibration response of layered, inhomogeneous regions with hard tumor inclusions and complicated boundary conditions set by the presence of skin, bones and other regions. An initial investigation has measured some tissue stiffness parameters, and applied these in a NASTRAN finite element analysis to simulate a prostate tumor in the pelvic cavity. The measurements show a wide separation between the elastic modulus of tumors and soft tissues such as muscle and prostate. NASTRAN analyses show the ability to delineate regions of different elasticity based on the pattern of vibration amplitudes. The ability to change vibration frequency within the 100–300 Hz band seems particularly helpful in simulations and experiments which visualize small stiff inclusions in tissues. Preliminary results support the postulate that sonoelasticity imaging can provide useful information concerning tissue properties that are not otherwise obtainable.

Key Words: **Sonoelasticity, Elastic constants, Young's modulus, Elasticity, Tissue characterization, Finite element analysis, Tumor detection.**

INTRODUCTION

Before the advent of modern medical imaging, palpation of hard masses was a primary screening technique for detection of malignant tumors. Today, palpation is still a widely used screening procedure for carcinomas of the breast, thyroid, and prostate. Malignant tumors are commonly encountered as hard masses within surrounding soft tissues, but detection by palpation is restricted to only these tumors which occur close to an accessible surface. In transrectal ultrasound B-scan imaging, palpable hard masses of the prostate may appear as hypoechoic, or hyperechoic, or isoechoic regions. Fundamentally, B-scan speckle brightness or echogenicity within a tissue is not related to tissue "hardness." For example, in medical ultrasound, the reflectivity of tissues is based on internal inhomogeneities or scatterers; wave equations are commonly cast in terms of fluid properties; and the wave propagation is at high frequencies (MHz). In contrast, since palpation is in some sense an evaluation of the bulk stiffness or hardness of a region, the appropriate model is a solid, and the "measurement" is low frequency (as compressional pulses are slowly applied). Our "sonoelasticity imaging" technique is an attempt to bridge the gap between low frequency hardness information and high frequency scattering images (Lerner and Parker 1987, 1988; Lerner et al. 1990). The technique combines externally applied vibrations with Doppler detection of the response throughout tissue, to indicate abnormal regions.

There has been consistent interest in tissue hardness, motion, and vibration over the years. Oestreicher and colleagues studied the physics of vibration in soft tissue, and showed that the impedance of tissue increases with frequency over audio frequencies, with the imaginary (reactive) part growing rapidly above 20 Hz and changing sign above 100 Hz (Von Gierke et al. 1952; Oestreicher 1951). Measurements of tissue elastic properties have been made, although wide ranges of values are reported, with muscle the most extensively reported and little or nothing on organs such as liver or prostate, and tumors (Fung 1981).

Address all correspondence to: Professor Kevin J. Parker, Department of Electrical Engineering, University of Rochester, Rochester, NY 14627.

Ultrasound detection of motion or compression, using autocorrelation or Doppler techniques has received recent attention (Tristam et al. 1986, 1988; Levinson 1987; Krouskop et al. 1987; Yamakoshi et al. 1988). However, major questions are still unanswered. For example, what are the material properties of soft tissues and tumors pertinent to sonoelasticity imaging, and what is the response of complex, layered tissues to applied vibrations given realistic boundary conditions? These questions are the key to optimizing the applied vibration frequency and source size, optimizing the Doppler detection and display algorithms, and determining the sensitivity and specificity of sonoelasticity imaging. This paper makes an initial contribution to the questions by reporting some preliminary measurements of tissue elastic constants, and using a NASTRAN finite element model to evaluate the theoretical response of a prostate in the pelvic cavity to applied vibration.

THEORY AND METHODS

Tissue stiffness

We begin by assuming an undeformed cubic element is loaded on its upper surface (Fig. 1), and supported at the base, with unconstrained sides. Then, with τ representing stress (force/area) and ϵ representing strain (fractional change in length for normal strains) we have the following conditions: τ_{xx}, ϵ_{xx}, ϵ_{yy}, ϵ_{zz} are nonzero, and τ_{yy}, τ_{zz}, τ_{xy}, τ_{xz}, τ_{yz}, ϵ_{xy}, ϵ_{yz}, ϵ_{xz} are zero.

Under these conditions the linear stress-strain equations reduce to:

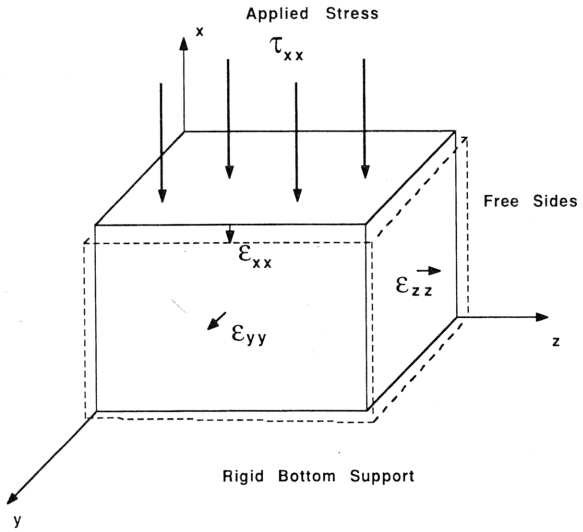

Fig. 1. Tissue model for stiffness measurements. The vertical deformation is measured with external stress applied on the top.

$$\epsilon_{xx} = \frac{1}{E}\tau_{xx} \tag{1}$$

and

$$\epsilon_{zz} = \epsilon_{yy} = \frac{-v}{E}\tau_{xx} \tag{2}$$

E and v are the Young's modulus (stiffness) and Poisson's ratio, respectively.

In principle, it is possible to apply a known load to a sample, and determine both E and v from measurements of strain using eqns (1) and (2). In practice, the transverse strain is difficult to measure accurately, and therefore, we have assumed a value of v for tissues of 0.495, close to incompressible (0.5) and approximately the value for water. The axial strain can be measured using the apparatus of Fig. 2. A sample is cut with a boring tube and surgical blades. The sample is placed on a triple beam balance and tared, using the sliding weight. Approximately 10 g of "preloading" is then added and the precision slide brought in contact with the sample and turned to restore the scale to equilibrium position. This is the starting point for force-displacement measurements. Next, force is added in regular increments by adjusting the sliding weight and the resulting compression is measured by moving the slide each time so as to restore the equilibrium position of the analytical balance. To convert these parameters to stress and strain, measurements of the cross-sectional area and height of the sample are obtained by micrometer readings. Typical measurements are shown in Fig. 3. The Young's modulus E can be estimated from the slope of these curves. Given the non-uniform nature of cut tissue, the dimension measurements introduce significant (±20%) error in the estimate of E. Furthermore, tissues exhibit nonlinear behavior and hysteresis effects at relatively small strains, thus the estimate of E depends on the history of the applied load, as shown in Fig. 3(b). Because our typical sonoelasticity imaging experiments utilize small (less than 0.5 mm) displacements at the vibration source, we have defined E to be the slope of the stress-strain curve near the origin, as derived from a second order polynomial fit to the compression curve of the initial loading.

NASTRAN model

A finite element analysis program NASTRAN (MacNeil-Schwindler Corp.) was used to evaluate a model of the anterior male pelvic cavity containing the prostate, with and without a firm 2 cm^3 tumor located so as to be somewhat recessed and beyond the

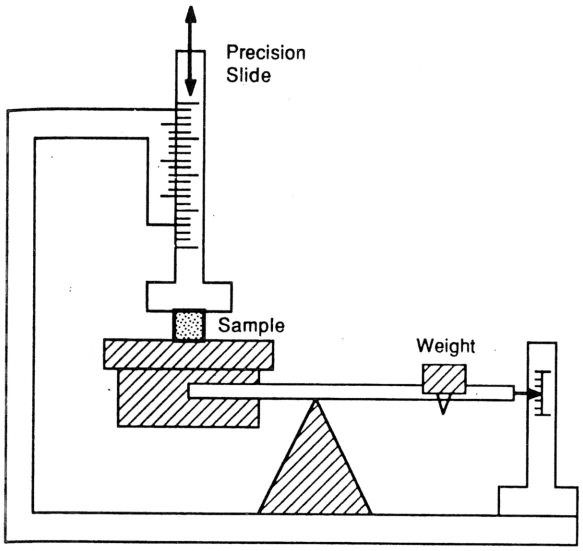

Fig. 2. Tissue stiffness measurement device. A specimen is supported on a triple beam balance, and is compressed from above by a precision slide.

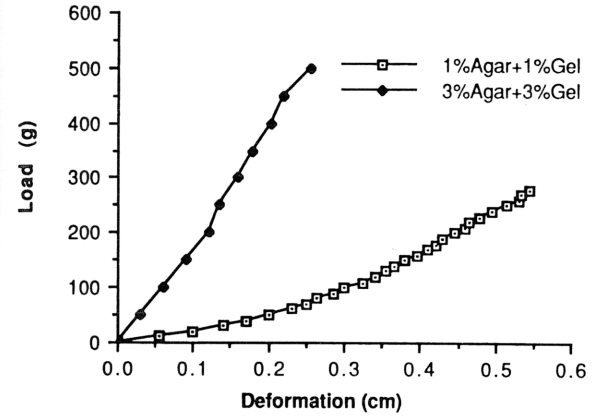

(a)

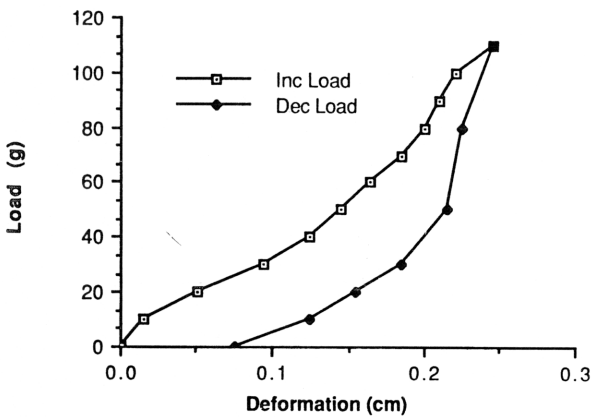

(b)

Fig. 3. (a) Stiffness measurements of agar-gelatin mixture. (b) Stiffness measurements of normal human prostate showing hysteresis effects.

region of easy digital palpation. Figure 4 shows the model consisting of a region of soft tissue surrounding an 18 cm^3 prostate which may contain a 2 cm^3 hard tumor. The prostate is centered vertically in the soft tissues, and is 1 cm back from the front facing wall of Fig. 4, which would correspond to the rectal wall. The back facing wall of Fig. 4 corresponds to the

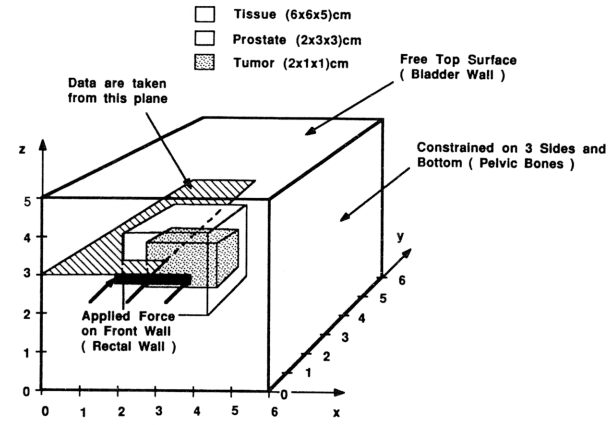

(a)

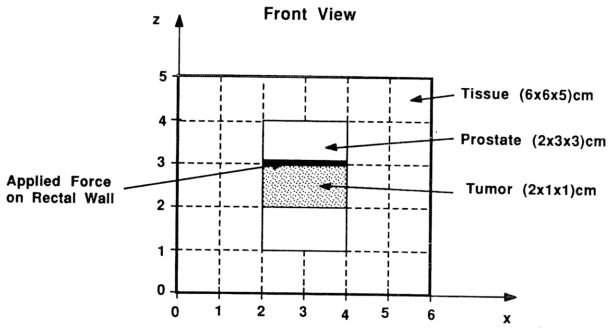

(b)

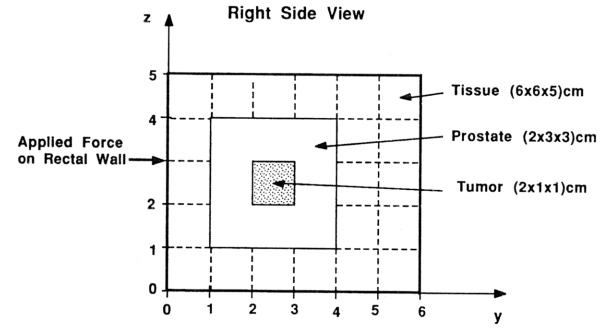

(c)

Fig. 4. (a) Three dimensional overview of the NASTRAN tissue-prostate-tumor model. A line force is applied on the front wall at $x = 2$–4, $y = 0$, $z = 3$ cm. The coordinates of the front, lower, left corner of prostate and tumor are (2, 1, 1) and (2, 2, 2), respectively. (b) Front view of the NASTRAN tissue model. (c) Right side view of the NASTRAN tissue model.

location of the symphysis pubis bone. The tumor is centered vertically and front-to-back within the prostate. Although not strictly representative of a peripheral prostatic carcinoma, the location and shape fit within the rectangular finite element grid, and represent the effect of a hard, nonpalpable inclusion on tissue vibration. Cubic finite elements 1 cm on each edge were used, and the total model consists of 180 connected elements. An applied sinusoidal force is placed on three nodes of the facing wall of Fig. 4, covering a region 3 cm long and 0.25 cm wide and representing a vibration source built into a transrectal sonoelasticity imaging probe. The assumptions and boundary conditions are: front facing wall (rectal wall), unconstrained or free surface except at the line of applied force; top wall (bladder boundary), unconstrained surface; three sides and bottom (connections to pelvic bone), constrained with zero translation surfaces. The NASTRAN program sets up the matrix equations balancing forces:

$$F_0 e^{j\omega_0 t} = \omega_0^2 MX + K(1 + j\gamma)X$$

where F is the applied force, M is the mass (inertial) terms, ω_0 the applied frequency, X displacements, γ the damping loss terms, and K the stiffness terms. The M matrix is derived from the density and size of each element, and the K matrix is derived from the elastic constants (stiffness or Young's Modulus and the Poisson's ration) of each material type. The γ damping matrix represents an imaginary component of stiffness. Without reliable measurements of damping in tissues, we have found that solutions are insensitive to γ in the 0.0 to 0.3 range. A value of 0.1 (10% imaginary component) was deemed reasonable and used in all subsequent simulations and was held constant over all frequencies. A solution yields the X, Y, and Z translations at each grid point, and for sinusoidal motion the velocity and translation are related by frequency, ω_0, so plots of vibration amplitude (translation) are directly related to plots of Doppler detected velocity (sonoelasticity images).

RESULTS AND DISCUSSION

Stiffness measurements

Measured values of E from compression experiments are given in Fig. 5. The shaded areas represent the range of all measured samples. The number of tissue specimens measured is given as N in the legend. Note the log scale of the vertical axis. Rubber values compare favorably with the literature (Crandall et al. 1978). Tissues are generally 1–3 orders of magnitude below the rubber, and this is somewhat consistent with the results of digital palpation. One caution is that the stiffness of tissues (excised) is measured at low strain levels, and since the tissues are highly nonlinear, the apparent stiffness increases sharply as increasing force is applied. Also as the tissues are excised, the effect if any of blood flow and normal blood pressure on the tissue stiffness in unknown. Another

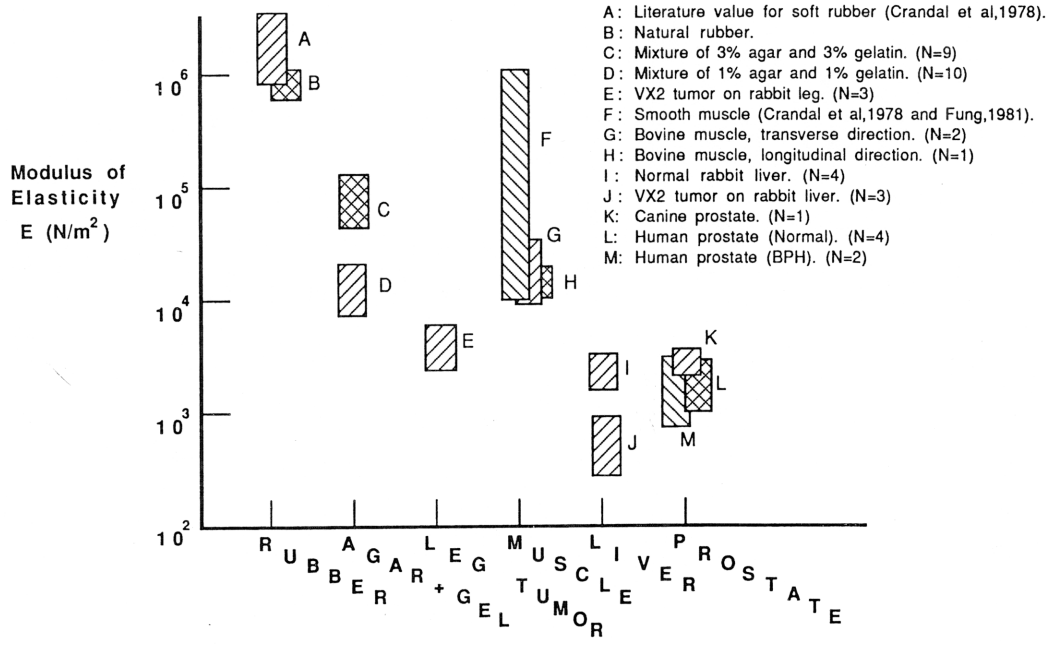

Fig. 5. Modulus of elasticity plotted in SI units, as measured for various specimens.

caution is that the values reported for VX2 tumors and prostate specimens are based on the overall response of inhomogenious specimens. For example, the VX2 tumors contain a palpably stiff perimeter and a relatively soft necrotic core, and the overall result is a low measured value of E. In the prostate, the peripheral gland and central zone are likely to have different properties. Measurements of smaller sections are desirable in these cases. Overall, Fig. 5 shows that tissue stiffness may be useful as a tissue characterization parameter, since good separation is found between tumors and other tissues.

NASTRAN results

Using our measurements and literature values as a guide, the NASTRAN model was programmed with values which are intended to represent phantom experiments shown in the companion paper (Lerner et al. 1990):

Tissue	Stiffness E Pascal (N/m^2)	Poisson's Ratio ν	Density ρ (gm/cm^3)
Soft-tissue	1.4×10^4	0.495	1.01
Prostate	2.8×10^4	0.495	1.02
Tumor	2.8×10^5	0.495	1.05

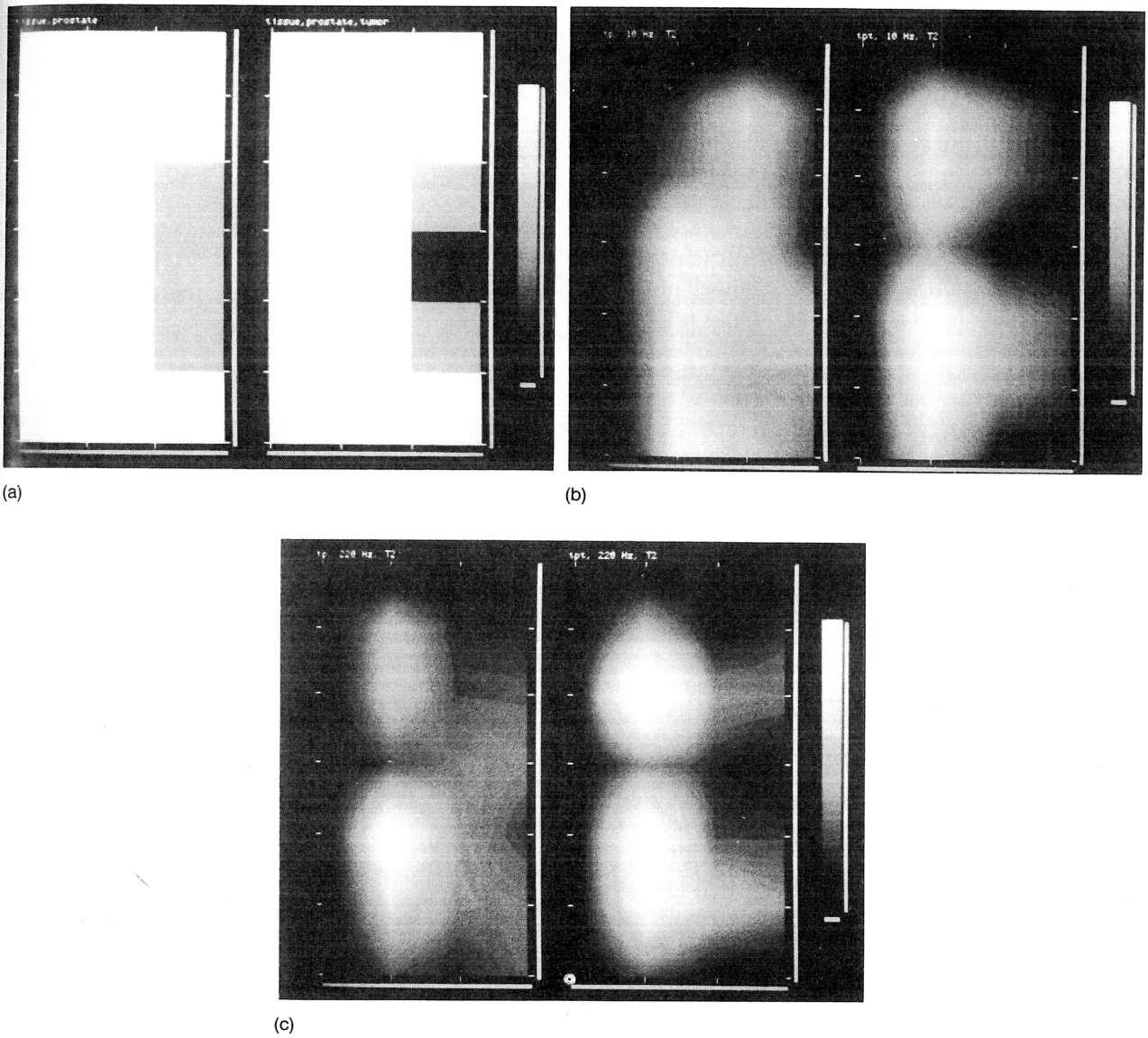

Fig. 6. Images showing vibrational amplitudes within the NASTRAN prostate model. Because of symmetry, only the left half of each model is shown. In (a) the geometry of the half-plane within each model is shown, on the left hand side is the normal prostate (gray). On the right is the model of the prostate with a stiff tumor (black). In (b) are the results from applied vibration at 10 Hz. Some effect of the tumor is seen on the right-hand model, but the definition is poor. In (c) are vibrations at 220 Hz, and relatively sharp demarcation of the prostate tumor are seen.

Solutions were obtained for frequencies between 10 and 910 Hz vibration applied to the rectal wall. Data are presented as a gray scale images, with white representing the highest vibrational response for that particular experiment and black representing zero vibration (translation). Linear interpolation is used to represent vibrational amplitudes between grid points. Only the y-axis vibrations are plotted, as a transrectal Doppler probe would only detect the component of motion along its axial direction, assumed to be aligned with the y-axis of Fig. 4. As the model is symmetric left to right, data are shown only for the left half side, and the vibrational amplitudes are shown for a horizontal plane which includes the applied force as shown in Fig. 4. These results, shown in Fig. 6, compare favorably with experimental sonoelasticity images of phantoms and tissues shown in the companion paper (Lerner et al. 1990). In general, the vibrational frequencies between 100 and 330 Hz produced best "definition" of tumor. Low frequency results, such as the 10 Hz data shown in Fig. 6, tend to have less differentiated patterns. Regions of high and low vibrations, presumably due to excitation of specific modes, could be seen at a number of frequencies. If these general results are found in practice, it will be necessary to sweep frequency in order to recognize a localized and consistent (over frequency) disturbance due to a region of abnormal elastic properties.

CONCLUSION

Preliminary results indicate that order-of-magnitude differences may exist between the stiffness of different tissue specimens, although localized measurements are needed in highly inhomogeneous samples such as VX2 carcinoma and the prostate. Furthermore, significant differences in vibrational velocities can be localized around cm-size regions of altered stiffness which are centimeter sized or less. This makes possible detection of tumors by sonoelasticity imaging, even though the tumors may not be apparent on conventional B-scan imaging. Additional work is required to determine the actual elastic constants of normal tissues and tumors, and also to evaluate experimentally and theoretically the response of these tissues to applied vibrations. Preliminary indications are that vibrational frequencies between 100–300 Hz will be most useful for discriminating between soft tissues and hard lesions, and that stiff lesions will be detectable at cm^3 volumes or less. These concepts may be useful for tumor detection in other organs such as breast, thyroid, and liver.

Acknowledgments—The authors are grateful for expert advice, insight and encouragement from Professor S. A. Gracewski. The tumor and tissue samples were provided through support from NIH Grant CA44732.

REFERENCES

Crandall, S. H.; Dahl, N. C.; Lardner, R. J. An introduction to the mechanics of solids, 2nd ed. New York: McGraw Hill Inc.; 1978:286.

Fung, Y. C. Biomechanics-mechanical properties of living tissues. New York: Springer-Verlag; 1981.

Krouskop, T. A.; Dougherty, D. R.; Levinson, S. F. A pulsed Doppler ultrasonic system for making non-invasive measurements of the mechanical properties of soft tissue. J. Rehabil. Res. Devel. 24:1–8; 1987.

Lerner, R. M.; Parker, K. J. Sono-elasticity imaging in ultrasonic tissue characterization and echographic imaging. In: Thyssen, J. M., ed. Proceedings of the 7th European Communities Workshop, October 1987, Nijmegen, The Netherlands. Luxembourg: European Communities.

Lerner, R. M.; Parker, K. J. Sono-elasticity imaging. In: Kessler, L. W., ed. Acoustic imaging. New York: Plenum Co.; 1988:317–327.

Lerner, R. M.; Huang, S. R.; Parker, K. J. "Sonoelasticity" images derived from ultrasound signals in mechanically vibrated tissues. Ultrasound Med. Biol. 16:231–239; 1990.

Levinson, S. F. Ultrasound propagation in anisotropic soft tissues: The application of linear elastic theory. J. Biomechanics 20:251–260; 1987.

Oestreicher, H. L. Field and impedance of an oscillating sphere in a visoelastic medium with an application to biophysics. J. Acoust. Soc. Am. 23:707–714; 1951.

Tristam, M.; Barbosa, D. C.; Cosgrove, D. O.; Nassiri, D. K.; Bamber, J. C.; Hill, C. R. Ultrasonic study of in-vivo kinetic characteristics of human tissues. Ultrasound Med. Biol. 12:927–937; 1986.

Tristam, M.; Barbosa, D. C.; Cosgrove, D. O.; Bamber, J. C.; Hill, C. R. Application of Fourier analysis to clinical study of patterns of tissue movement. Ultrasound Med. Biol. 14:695–707; 1988.

Von Gierke, H. E.; Oestreicher, H. L.; Franke, E. K.; Parrack, H. O.; Wittern, W. W. Physics of vibrations in living tissues. J. Appl. Physiol. 887–900; 1952.

Yamakoshi, Y.; Morri, E.; Sato, T. Imaging of precise movement of soft tissue for forced vibration. In: Linzer, M., ed. 13th International Symposium on Ultrasonic Imaging and Tissue Characterization, June 6–8, 1988, Arlington, VA. New York: Academic Press, Inc.